Journal of Molecular Modeling (2019) 25: 219
https://doi.org/10.1007/s00894-019-4089-1

ORIGINAL PAPER

Triel bonds in $RZH_2\cdots NH_3$: hybridization, solvation, and substitution

Zhefeng Xu[1] · Yan Li[1]

Received: 6 March 2019 / Accepted: 4 June 2019 / Published online: 12 July 2019

Abstract

The influence of hybridization, substitution, and solvation on the triel bond has been investigated in the complexes of $RZH_2\cdots NH_3$ (Z = B and Al). The magnitude of the π-hole on the triel atom is related to the nature of the Z atom and the hybridization of R. CH_3BH_2 has the largest π-hole among RBH_2, while for $RAlH_2$ the largest π-hole is found in $CH{\equiv}CAlH_2$. The interaction energy is partly inconsistent with the magnitude of the π-hole on the triel atom and the orbital interaction from the N lone pair of NH_3 into the empty p orbital of the triel atom. The strongest B···N triel bond is found in $CH{\equiv}CBH_2\cdots NH_3$, while the weakest Al···N triel bond is in $CH_3AlH_2\cdots NH_3$. The strength of the triel bond is increased in solvents, and its enhancement is prominent with the increase of solvent polarity. Solvents also change the nature of the Al···N triel bond from an electrostatic interaction to a partially covalent one. The F substituent in the triel donor strengthens the triel bond, depending on the substitution position and number.

Keywords Triel bonding · Hybridization · Substituents · Solvents

Introduction

Different Lewis acid–base interactions are ubiquitous in various chemical, physical, and biological processes [1, 2]. Owing to the diversity of Lewis acid centers, these Lewis acid–base interactions are diverse, including hydrogen, halogen, and tetrel bonds, but most of them can be classified as σ-hole bonds [3–5]. The σ-hole is a region of depletion of the electron in the outer lobe of the half-filled p orbital that is involved in a covalent bond [3–5]. Another type of Lewis acid–base interaction is a π-hole bond, where the π-hole is a region of electron deficiency situated in a direction perpendicular to a center of a planar portion of a molecular framework [6–8]. An interesting issue is to compare the strength of σ-hole and π-hole bonds in different systems [9–12]. It was concluded that in most cases the π-hole bond is stronger than the σ-hole bond. This has an important implication in molecular recognition since the latter is partly dependent on the interaction strength. It was demonstrated that the π-hole bonds play important roles in crystal engineering [14] and biological systems [15, 16]. Therefore, more attention was paid to the π-hole bonds particularly those involving the C=O group [17–20]. Another usual π-hole bond is the triel bond, which is an attractive and highly directional Lewis acid–base interaction between a π-hole on the group III atom and a Lewis base [21]. Previously, complexes combined by this interaction were called partially bonded complexes since their binding distances are in the intermediate range between a van der Waals interaction and a covalent bond [22]. It should be noted that a triel atom also provides a σ-hole if it is bonded with four atoms or groups [23].

There are many theoretical and experimental studies on triel bonding [24–34] because it is involved in some important chemical processes particularly in the release of molecular hydrogen in hydrogen storage materials [35, 36]. Besides molecules with lone pairs, π systems [37, 38], metal hydrides [30, 39], and radicals [13] also engage in a triel bond. Some previous studies focused on the condensed-phase effects on the structural properties in triel-bonded complexes with experimental and theoretical methods [24, 27]. This is because triel bonding shows some abnormal larger shortening in the binding distance when it combines with another weak interaction [40]. On the other hand, triel bonding can compete with other types of interactions. For example, BX_3 (X = F, Cl, Br, and I) can participate in lone pair···π, halogen···π, and triel bonding

✉ Yan Li
yanli_sub@163.com

[1] Department of Chemical Engineering, Inner Mongolia Vocational College of Chemical Engineering, Hohhot 010070, People's Republic of China

interactions with ethene, 1,2-difluoroethene, and perfluoroethene, but triel bonding dominates over the other two interactions [41].

The strength of a Lewis acid–base interaction is affected by factors other than the nature of both the Lewis acid and base, such as hybridization, solvation, and substitution. Usually, when the hybridization of R adjoined to the Lewis acid varies from sp^3 to sp^2 to sp, the stronger interaction is obtained. This conclusion has been confirmed in the C–H···Y (Y is a Lewis base) hydrogen bond [42–44], C–X···Y (X = halogen) halogen bond [45], and C–SiF_3···NH_3 tetrel bond [10]. Solvents have complicated effects on the strength of a Lewis acid–base interaction, which is dependent on the type and strength of this interaction as well as the polarity of solvent [46–48]. Theoretical studies showed that increasing the polarity of solvent leads to strengthened halogen bonding and weakened hydrogen bonding [46]. Then experimental evidence confirmed that hydrogen-bonded co-crystals are favorable in less polar solvents, while halogen-bonded co-crystals in more polar solvents [47]. This switching by solvents depends on the relative strengths of both interactions [47]. Very recently, a theoretical study unveiled the mechanism of solvent effect on the strength of halogen bond [48]. Su and co-authors thought that the influence of solvent on the strength of halogen bond is mainly realized by modulating its polarization contribution since polarization is more sensitive to the solvent effects than the other interaction terms [48]. F substitution in a Lewis acid would enhance the strength of hydrogen bond [49], halogen bond [50], and tetrel bond [10]. Thus, there appears an issue: How do the hybridization, solvent, and substituent influence the strength and nature of triel bonding?

In this study, we selected RZH_2···NH_3 (Z = B and Al) as a model to investigate the effect of hybridization on the strength of triel bonding. These complexes were also explored in solvents (heptanes and dimethyl sulfoxide (DMSO)) to study the effect of solvents on the strength and nature of triel bonding. From CH_2=$CHZH_2$···NH_3, the hydrogen atoms of the CH_2=CH group were replaced by different numbers of F atoms to probe the substitution effect on the strength of triel bonding. These complexes were investigated in view of geometrics, interaction energy, charge transfer, orbital interactions, and electron density.

Computational details

The structures of the monomers and complexes were first optimized at the MP2/aug-cc-pVDZ level. Frequency calculations at the same level confirmed that all structures are energetic minima since no imaginary frequencies were observed. These structures were then re-optimized at the MP2/aug-cc-pVTZ level to obtain more accurate results. The interaction energies (ΔE) were calculated as differences between the energy of the complex and the sum of energies of monomers with their geometries in the complex, and they were corrected for the basis set superposition error (BSSE) by the counterpoise method [51]. All calculations were carried out within the framework of the Gaussian 09 set of codes [52].

The atoms in molecules (AIM) analysis was used to find the intermolecular bond critical points (BCPs) and to calculate the corresponding topological parameters, including electron density, its Laplacian, and total energy density. The AIM analyses were performed with the use of the AIM2000 program [53]. The molecular electrostatic potentials (MEPs) of the isolated monomers have been analyzed with the Wave Function Analysis-Surface Analysis Suite (WFA-SAS) program [54] on the 0.001 a.u. electron density isosurface. The natural bond orbital (NBO) method [55] implemented in Gaussian 09 was applied to analyze orbital interactions and charge transfer at the HF/aug-cc-pVTZ level. The localized molecular orbital-energy decomposition analysis (LMO-EDA) method [56] was used to decompose the interaction energy of the complex using the GAMESS program [57] at the MP2/aug-cc-pVTZ level. An analysis of natural orbital for chemical valence (NOCV) was performed at the GGA-BPE-D3/QZ2P level with the ADF program [58].

Results and discussion

MEPs

An analysis of MEP can provide some useful information for interaction sites between two molecules and the corresponding interaction strength. Figure 1 illustrates the MEP maps on the 0.001 au molecular surfaces of monomers. Obviously, two red areas with positive MEPs (π-holes) are found on the triel atom, and their maximal values are also marked in Fig. 1. The heavier triel atom has the bigger π-hole than the lighter analogue due to its larger polarization and less electronegativity. Thus, these π-holes act as a Lewis acid to bind with a base such as NH_3. When the hybridization of the triel atom is varied, the π-hole is biggest in CH≡$CAlH_2$ (CH_3BH_2) but smallest in CH_2=$CHZH_2$. The biggest π-hole in CH≡$CAlH_2$ can be attributed to the greatest electronegativity of the acetenyl group, while both the biggest π-hole in CH_3BH_2 and the smallest one in CH_2=$CHZH_2$ cannot be explained with electronegativity since the vinyl group has greater electronegativity than the methyl group.

How are these unexpected variations for the MEPs on these triel atoms explained? We fall back on orbital interactions in these molecules. In CH_2=$CHZH_2$, a conjugative effect occurs between the π electrons on the C=C bond and the empty p orbital of the triel atom, confirmed by an orbital interaction from the π occupied orbital to the empty p orbital. The corresponding perturbation energy is 36.48 and 13.90 kcal mol^{-1} in

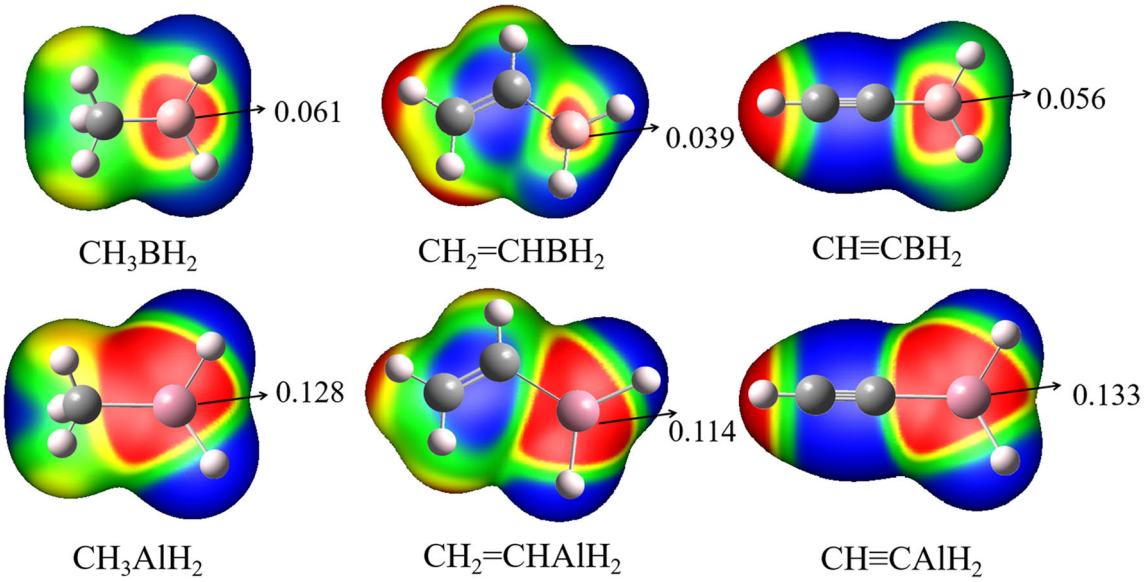

Fig. 1 MEP maps of the monomers on the 0.001 a.u. electron density isosurface. Color ranges, in au, are: red, greater than 0.0193; yellow, between 0.0193 and 0.0108; green, between 0.0108 and −0.0030; and blue, less than −0.0030

CH_2=$CHBH_2$ and CH_2=$CHAlH_2$, respectively. A similar orbital interaction is also present in CH≡CZH_2 and the respective perturbation energy is 28.70 and 8.25 kcal mol^{-1} in CH≡CBH_2 and CH≡$CAlH_2$. Another type of conjugative effect between the C–H σ orbital and the empty p orbital of the triel atom is present in CH_3BH_2 and CH_3AlH_2 with the perturbation energy of 17.83 and 4.49 kcal mol^{-1}. Such conjugative effect results in an increase of electron density on the triel atom and thus a smaller π-hole. It is found that the conjugative effect is more prominent in RBH_2 than that in $RAlH_2$. For a given triel center, the conjugative effect is dependent on its hybridization, bigger from sp^3 to sp to sp^2. The largest conjugative effect in CH_2=$CHZH_2$ is responsible for the smallest π-hole on the Z atom. Therefore, the magnitude of π-hole on the triel atom is a combinative result of the electronegativity of its adjoining group and the conjugative effect. In addition, it should be noted that positive electrostatic potential reflects the lower electronic density of the σ-hole as well as contributions from other portions of the molecule [59].

The MEP on the π-hole of BH_3 and AlH_3 is respectively 47.1 and 87.3 kcal mol^{-1} [13], which is larger than that in RZH_2. This means that the alkyl group plays an electron-donating role in RZH_2 and thus decreases its positive MEPs. If R is combined with a halogen atom, the positive MEP on the halogen atom increases from sp^3 to sp^2 to sp, which is different from that on the triel atom.

Hybridization

Figure 2 shows the optimized structures of the dyads with the binding distances. The binding distances are in the range of 1.648~1.660 Å and 2.057~2.076 Å in the B and Al complexes, respectively, which are much shorter than the sum of the van der Waals (vdW) radii of the corresponding atoms (3.4 Å for B and N; 3.7 Å for Al and N) [60]. The binding distance in the B complex is shorter from CH_2=$CHBH_2$···NH_3 to CH_3BH_2···NH_3 to CH≡CBH_2···NH_3, while the binding distance in the Al complex is shorter from CH_3BH_2···NH_3 to CH_2=$CHBH_2$···NH_3 to CH≡CBH_2···NH_3. Both of them are partly consistent with the positive MEP on the π-hole of RZH_2.

One also finds that the planar structure of the triel center is distorted in the complex. This deformation can be estimated with deformation energy in Table 1. The deformation energy is defined as the energy difference between the isolated molecules and the molecules at the geometry of the complex. This term in the B complex is three times larger than that in the Al counterpart. Thus, the deformation has a larger contribution to the stability of the B complex.

From Table 1, it is seen that the interaction energy of the B complex depends on the B hybridization, being more negative from sp^2 to sp^3 to sp, while the interaction energy of the Al complex is also largest in CH≡$CAlH_2$···NH_3 but is almost equal in CH_3AlH_2···NH_3 and CH_2=$CHAlH_2$···NH_3. The interaction energy in the B complex is more negative than that in the Al analogue, inconsistent with the positive MEP on the π-hole of RZH_2. This abnormal result is primarily attributed to the larger deformation energy in the B complex. The interaction energies of BH_3···NH_3 and AlH_3···NH_3 were calculated to be −40.09 and −32.87 kcal mol^{-1}, respectively, which are more negative than that in CH≡CZH_2···NH_3 but less negative than that in CH_3ZH_2···NH_3 and CH_2=$CHZH_2$···NH_3. Obviously, only the former result is consistent with the positive MEP of the π-hole of the triel atom.

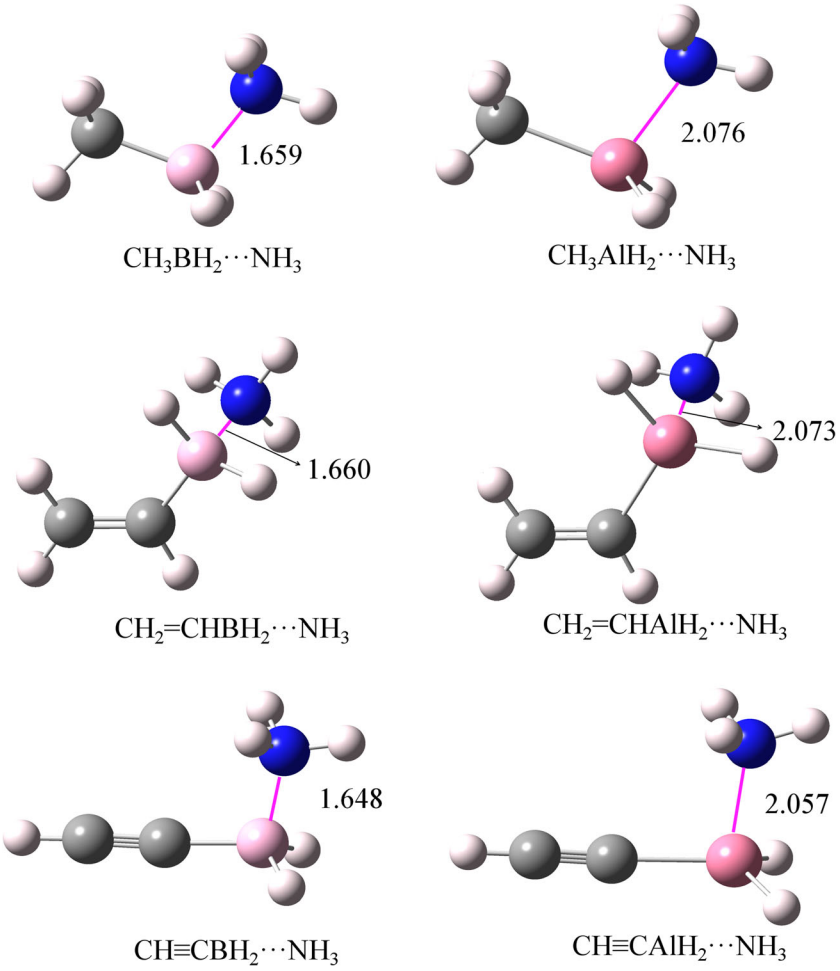

Fig. 2 The optimized structures of the dyads and binding distances are given in angstrom

The formation of triel bonding leads to a big charge transfer within 0.14–0.38e, which is partly due to the large distortion of RZH_2. The charge transfer in the B complex is bigger than that in the Al analogue, consistent with the interaction energy; specifically, the charge transfer in the B complex is more than twice that in the Al complex. However, the interaction energy in the former is one time larger than that in the latter. On the other hand, the charge transfer becomes bigger from $CH_3ZH_2\cdots NH_3$ to $CH_2{=}CHZH_2\cdots NH_3$ to $CH{\equiv}CZH_2\cdots NH_3$. This order is in line with the interaction energy in the Al complex but some inconsistencies are found between them in the B complex.

Intermolecular orbital interactions were not discerned in NBO calculations; thus, their contribution was analyzed by natural orbital for chemical valence (NOCV) with the ADF program. Red and blue areas represent charge density decrease and increase, respectively. According to the color of deformation densities in Fig. 3, charge shifts from the N atom

Table 1 Interaction energy (**Δ**E, kcal mol^{-1}), deformation energy (DE, kcal mol^{-1}), charge transfer (Q_{CT}, e), electron density (ρ, au), Laplacian (∇^2_{BCP}, au), and energy density (H, au) at the bond critical point

dyads	ΔE	DE	Q_{CT}	ρ	$\nabla^2\rho$	H
$CH_3BH_2\cdots NH_3$	−39.31	−12.58	0.3463	0.0997	0.5134	−0.0570
$CH_2{=}CHBH_2\cdots NH_3$	−38.58	−13.06	0.3539	0.1004	0.5037	−0.0585
$CH{\equiv}CBH_2\cdots NH_3$	−44.49	−13.07	0.3744	0.1057	0.4943	−0.0651
$CH_3AlH_2\cdots NH_3$	−31.36	−3.41	0.1429	0.0475	0.2871	0.0015
$CH_2{=}CHAlH_2\cdots NH_3$	−31.43	−3.51	0.1433	0.0481	0.2859	0.0011
$CH{\equiv}CAlH_2\cdots NH_3$	−35.12	−3.73	0.1521	0.0504	0.3041	0.0007

Note: Q_{CT} is the sum of charge on all atoms of RZH_2.

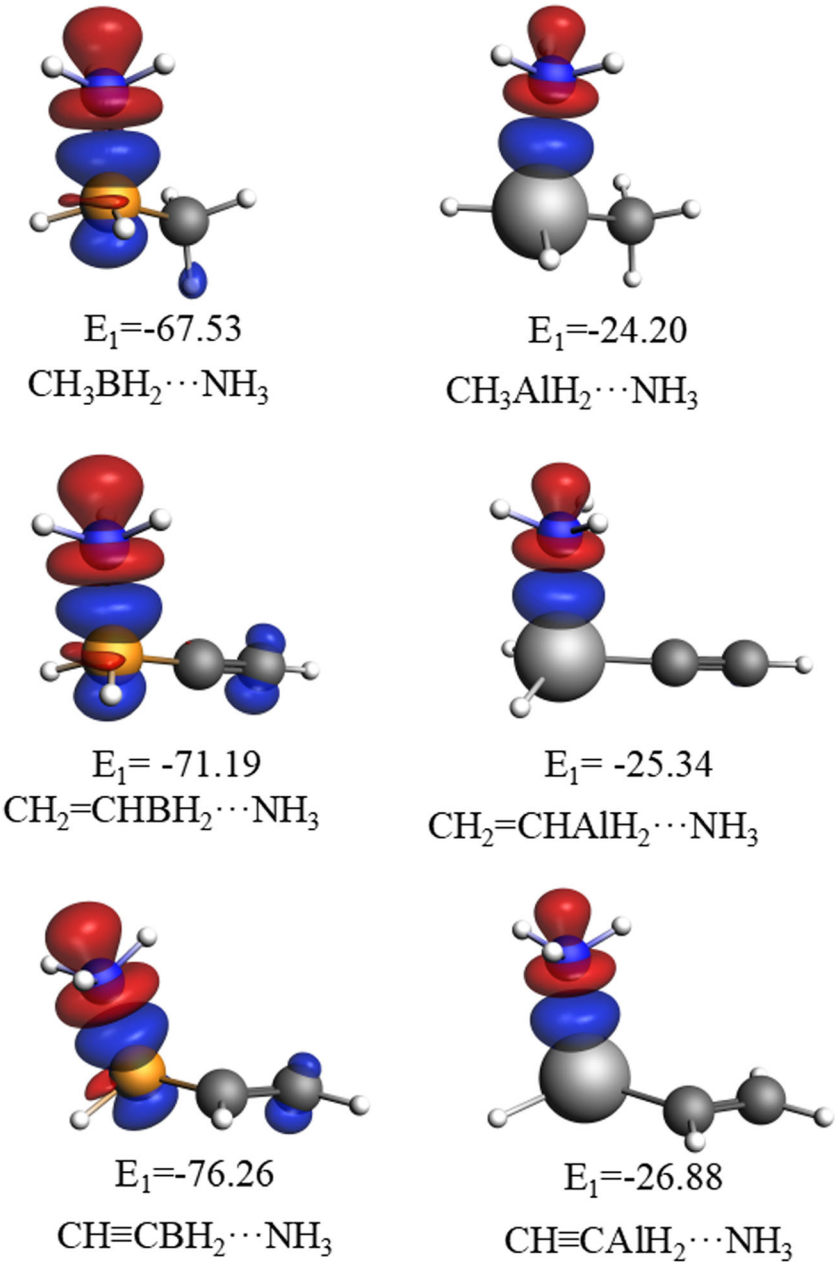

Fig. 3 Deformation densities of the pair-wise orbital interactions in the dyads at the GGA-BPE-D3/QZ2P//MP2/aug-cc-pVTZ level. The associated orbital interaction energies are given in kcal mol^{-1}. The color code of the charge flow is red–blue and the isovalue is 0.005 au

into the triel atom in all interactions. From the shape of deformation densities, we think that an orbital interaction between the lone pair orbital on the N atom and the empty p orbital of the triel atom is present. This orbital interaction contribution increases from sp^3 to sp^2 to sp, and its value in the B complex is almost triple that in the Al complex.

An AIM analysis can be used to predict the presence of an interaction and to estimate its strength and type. A bond critical point (BCP) is present between the Z and N atoms, and its electron density, Laplacian, and total energy density are given in Table 1. For a given Z···N interaction, the electron density also varies with the hybridization of R, being larger from sp^3 to sp^2 to sp. The value of Laplacian is positive for all complexes, indicating the electron density is depleted at the Z···N BCP. However, the sign of energy density varies dependent on the nature of the triel atom. That is, it is positive in the Al complex but is negative in the B complex. According to the proposition of Koch and Popelier [61], the B···N interaction has a partially covalent character, while the Al···N interaction is basically electrostatic in nature.

In order to further explore the nature of the triel bond, we divided the interaction energy into five parts in Table 2: electrostatic energy (E^{ele}), exchange energy (E^{ex}), repulsion energy (E^{rep}), polarization energy (E^{pol}), and dispersion energy (E^{disp}). E^{ele} is defined as the Coulomb energy between the two unperturbed partners, E^{ex} is chiefly caused by the overlap

Table 2 Electrostatic energy (E^{ele}), exchange energy (E^{ex}), repulsion energy (E^{rep}), polarization energy (E^{pol}), and dispersion energy (E^{disp}); all energies are in kcal mol^{-1}

dyads	E^{ele}	E^{ex}	E^{rep}	E^{pol}	E^{disp}
$CH_3BH_2\cdots NH_3$	−82.86(51.5%)	−129.93	250.23	−66.94(41.6%)	−11.06(6.9%)
$CH_2{=}CHBH_2\cdots NH_3$	−86.60(51.4%)	−137.81	266.20	−70.66(42.0%)	−11.11(6.6%)
$CH{\equiv}CBH_2\cdots NH_3$	−90.44(51.2%)	−137.91	268.69	−75.94(43.0%)	−10.26(5.8%)
$CH_3AlH_2\cdots NH_3$	−59.51(67.3%)	−57.78	113.98	−25.67(29.0%)	−3.30(3.7%)
$CH_2{=}CHAlH_2\cdots NH_3$	−61.37(66.8%)	−61.44	120.86	−26.92(29.3%)	−3.61(3.9%)
$CH{\equiv}CAlH_2\cdots NH_3$	−64.36(67.0%)	−60.26	120.19	−28.78(29.9%)	−2.97(3.1%)

Note: The percentage of each term relative to the sum of E^{ele}, E^{pol}, and E^{disp} is given in parentheses.

of molecular orbitals, E^{rep} mainly originates from Pauli repulsion, E^{pol} is defined as the energy lowering due to the intramolecular relaxation of each molecule's ALMOs in the field of all other molecules in the system, and E^{disp} is derived via a supermolecule approach using size-consistent correlation methods, such as MP2 and CCSD(T). The exchange energy is much larger than the electrostatic energy in the B complex, while both terms are almost equal in the Al complex. Because the repulsion energy depends on the exchange energy and they cancel each other, we do not focus on both terms. Considering the B···N interaction or the Al···N interaction, three attractive terms (E^{ele}, E^{pol}, and E^{disp}) are more negative from electrostatic to polarization to dispersion, as shown in Fig. 4. The electrostatic energy is about twice that of the polarization energy in the Al···N interaction; thus, this triel bond is electrostatically dominated. For the B···N interaction, electrostatic and polarization energies are comparable; thus, this interaction is mainly determined by a combination of electrostatic and polarization.

In the B complexes, the relatively larger E^{pol} means that the shape of the orbitals has undergone a large change, which is consistent with the deformation of the RBH_2 molecule. Both E^{ele} and E^{pol} are more negative from sp^3 to sp^2 to sp, while E^{disp} has a slight change with the hybridization. Each term in the B complex is greater than that of the Al complex and their largest difference is found for E^{pol}, indicating the boron atom is more easily polarized. Politzer et al. [62] pointed out that noncovalent interactions are Coulombic, with inclusion of polarization and dispersion, and thus the above energy decomposition analysis is necessary.

Solvent effect

It is interesting to study the strength of triel bonding in solvents; thus, we placed the six complexes above into two solvents of heptane and DMSO. Table 3 presents the changes of binding distance, charge transfer, and electron density in the

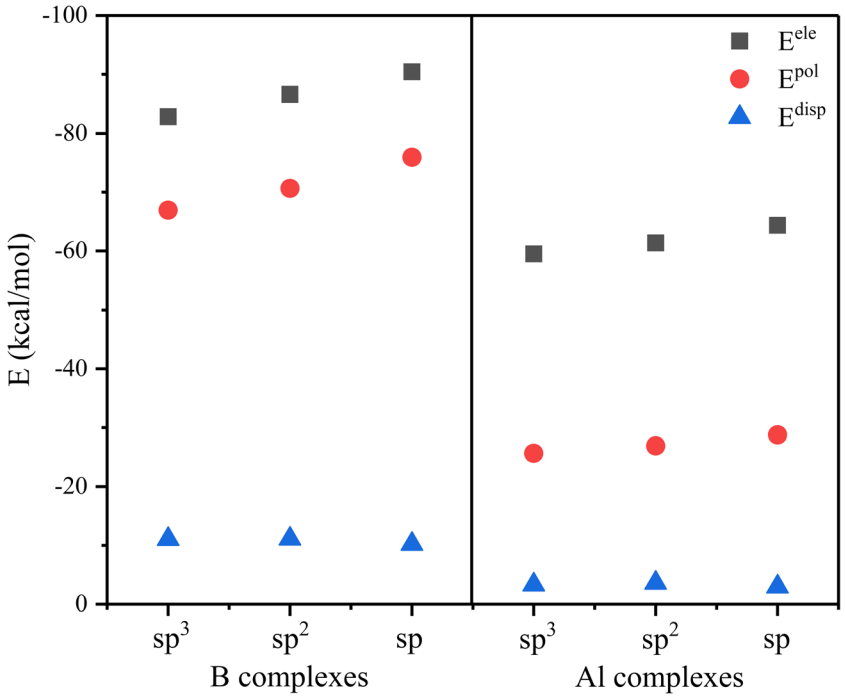

Fig. 4 Dependence of energy components on the hybridization of carbon atom adjoined to the triel atom

solvent relative to in the gas phase. The binding distance is shortened and charge transfer and electron density are increased, indicating that the triel bond is strengthened in solvents. This is because the B and Al atoms are easily polarized by solvents and thus engage in a stronger triel bond. Moreover, these changes are prominent with the increase of solvent polarity. Although the shortening of the binding distance is greater in the Al complex than that in the B analogue, both charge transfer and electron density have a larger increase in the latter complex. As a result, the B···N treil bond is greatly enhanced in the solvent relative to the Al···N treil bond. Here the binding distance does not truly reflect the strength of the triel bond in some cases, which supports the conclusion that close contacts between atoms are not always a reliable indicator of the actual interactions [63].

In both solvents, the binding distance shortens and electron density increases from sp^3 to sp^2 to sp for either the B complex or the Al complex, indicating that the strength of triel bond is stronger following the same order, which is different from that in the gas phase. Obviously, solvation has an important effect on the strength of the triel bond. With enhancement of the triel bond, its type is also varied. The energy density is from one positive value in the gas phase to a negative value in the solvent, becoming a partially covalent interaction.

Influence of F substitution

In this section, CH_2=$CHZH_2$···NH_3 (Z = B, Al) was chosen to study the influence of F substituents on the strength of triel bonding, where different sites of H atoms in CH_2=$CHZH_2$ are replaced by F substituents. Figure 5 shows the optimized structures of F derivatives of CH_2=$CHZH_2$···NH_3 (Z = B, Al). For simplicity, the F derivatives of CH_2=$CHZH_2$···NH_3 are denoted as nF-Z, where Z denotes a triel atom (B or Al) and n is the number of F substituents (1–3). If one F substitution happens at the C position adjoined with the $–ZH_2$ group, NH_3 is inclined to approach the triel atom along the side of this F substitution since it is favorable for the attractive interaction between the F atom and the NH group. Otherwise, NH_3 attacks the triel atom from the opposite side in 1F-Z-b and 2F-Z-a, which is due to the presence of attractive interactions between the F atom at the terminal C atom and NH group. There is one exception in 1F-Z-a, where its conformation is like that in CH_2=$CHZH_2$···NH_3. Clearly, the C–C–Z–H dihedral angle has a prominent change in most complexes excluding 1F-Z-a relative to the unsubstituted complex. It is noted that we tried to make the conformations of F derivatives of CH_2=$CHZH_2$···NH_3 (Z = B, Al) uniform, but they change again into the ones shown in Fig. 5.

Owing to the electron-withdrawing property, the F substitution results in an increase of the positive MEP on the π-hole of the triel atom (Table 4). Generally, the triel atom has a larger MEP with an increase in F number. Moreover, the F substitution at the CH position causes a larger increase in the positive MEP than that at the CH_2 position. In addition, the F substitution has the same effect on the π-hole of both B and Al atoms.

Relative to CH_2=$CHZH_2$···NH_3, the Z···N distance is shortened owing to the F substitution. However, no good linear relationship is found between the Z···N distance and the positive MEP on the triel atom. For example, 1F-Al-b has the shorter Al···N distance but the smaller positive MEP on the Al atom than 1F-Al-a. Such inconsistency may be due to the cooperativity between the triel bond and the F···H secondary interaction as well as the conformation difference. Similarly, the interaction energy is increased owing to the F substitution, and the increase of interaction energy shows some inconsistencies with the positive MEP on the triel atom. In addition, the stronger triel bond is partly attributed to the increase of charge transfer. Thus, we think that the triel bond should be understood with a combination of electrostatic and orbital interactions.

Table 3 Changes in the binding distance (ΔR, Å), charge transfer (ΔQ_{CT}, e), and electron density (Δρ, au) of complexes in the solvent relative to the gas phase as well as the electron density (ρ, au) and energy density (H, au) in the solvent

		R	ΔR	ΔQ_{CT}	ρ	Δρ	H
Heptane	CH_3BH_2···NH_3	1.647	−0.012	0.0166	0.1045	0.0048	−0.0726
	CH_2=$CHBH_2$···NH_3	1.647	−0.012	0.0174	0.1054	0.0049	−0.0741
	CH≡CBH_2···NH_3	1.636	−0.012	0.0178	0.1107	0.0051	−0.0818
	CH_3AlH_2···NH_3	2.056	−0.020	0.0112	0.0506	0.0031	−0.0011
	CH_2=$CHAlH_2$···NH_3	2.053	−0.020	0.0121	0.0511	0.0031	−0.0015
	CH≡$CAlH_2$···NH_3	2.038	−0.019	0.0121	0.0535	0.0031	−0.0023
DMSO	CH_3BH_2···NH_3	1.629	−0.030	0.0439	0.1126	0.0129	−0.0626
	CH_2=$CHBH_2$···NH_3	1.628	−0.032	0.0460	0.1137	0.0132	−0.0640
	CH≡CBH_2···NH_3	1.618	−0.030	0.0463	0.1190	0.0134	−0.0712
	CH_3AlH_2···NH_3	2.022	−0.053	0.0320	0.0561	0.0086	−0.0015
	CH_2=$CHAlH_2$···NH_3	2.019	−0.053	0.0328	0.0568	0.0087	−0.0011
	CH≡$CAlH_2$···NH_3	2.005	−0.051	0.0329	0.0593	0.0089	−0.0003

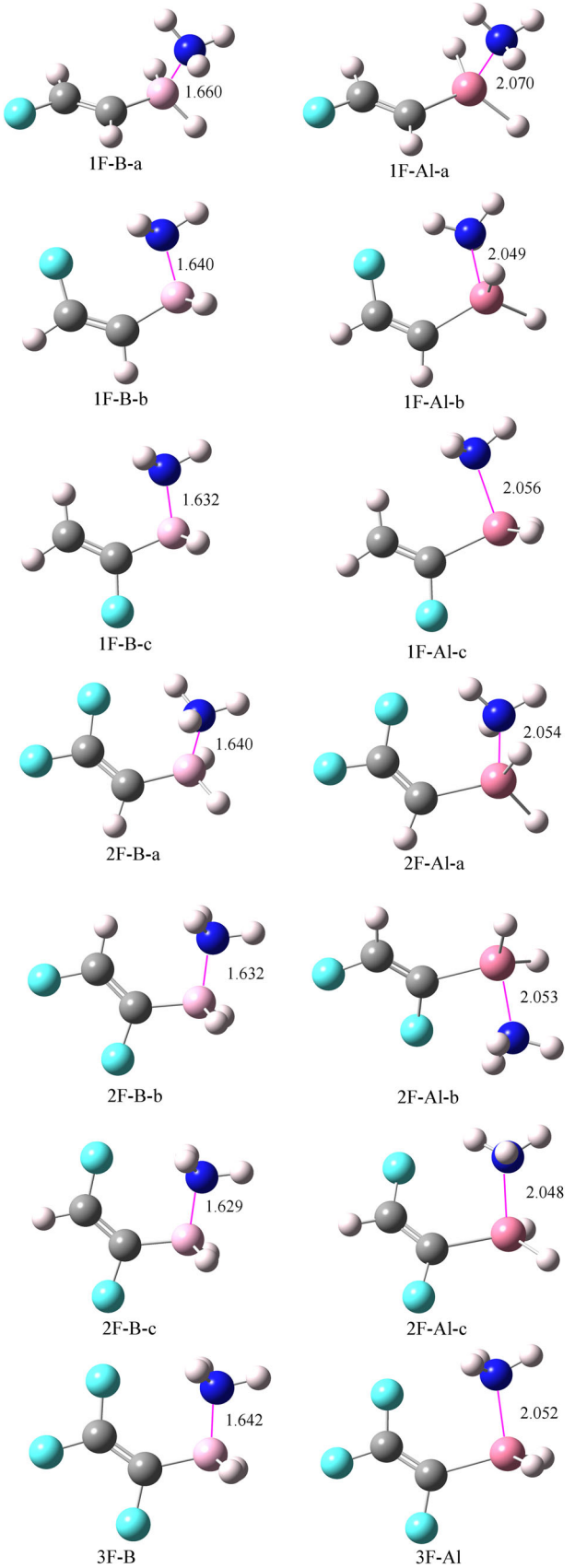

Fig. 5 The optimized structures of F derivatives of CH_2=$CHZH_2$···NH_3 (Z = B, Al).

Table 4 Interaction energy (ΔE, kcal mol^{-1}), binding distance (R, Å), charge transfer (Q_{CT}, e) in the F-substituted complexes and their difference (Δ) relative to the unsubstituted complexes as well as the most positive MEP on the π-hole of the Z atom (V_{max}, kcal mol^{-1}) in the F-substituted molecules

Dyads	ΔE	ΔΔE	R	ΔR	Q_{CT}	ΔQ_{CT}	V_{max}
1F-B-a	−38.69	−0.11	1.659	−0.001	0.3549	0.0010	27.07
1F-B-b	−51.15	−12.57	1.636	−0.024	0.3758	0.0219	27.32
1F-B-c	−48.64	−10.06	1.642	−0.018	0.3732	0.0193	34.11
2F-B-a	−45.73	−7.15	1.644	−0.016	0.3684	0.0145	28.83
2F-B-b	−45.07	−6.49	1.645	−0.015	0.3724	0.0185	34.73
2F-B-c	−48.19	−9.61	1.644	−0.016	0.3740	0.0201	35.17
3F-B	−46.95	−8.37	1.646	−0.014	0.3727	0.0188	35.68
1F-Al-a	−32.50	−1.07	2.069	−0.004	0.1454	0.0021	75.94
1F-Al-b	−37.33	−5.90	2.049	−0.024	0.1514	0.0081	75.69
1F-Al-c	−38.24	−6.81	2.053	−0.020	0.1522	0.0089	81.28
2F-Al-a	−36.40	−4.97	2.054	−0.019	0.1512	0.0079	78.20
2F-Al-b	−38.32	−6.89	2.053	−0.020	0.1531	0.0098	83.73
2F-Al-c	−38.45	−7.02	2.054	−0.019	0.1518	0.0085	83.79
3F-Al	−38.76	−7.33	2.053	−0.020	0.1528	0.0095	85.42

Conclusions

We performed theoretical calculations for the complexes of CH_3ZH_2···NH_3, CH_2CHZH_2···NH_3, and $CHCZH_2$···NH_3 (Z = B and Al) in view of the geometrics, energies, charge transfer, orbital interactions, and AIM analyses. The main conclusions are summed up as follows:

(1) The positive MEP on the π-hole of the triel atom in RZH_2 is related to the carbon hybridization of alkyl group R. It is larger in the order of $sp^2 < sp < sp^3$ for the B atom but $sp^2 < sp^3 < sp$ for the Al atom. This is a combinative result of the electronegativity of R and the conjugative effect.

(2) The triel bond is stronger in the sequence of $sp^2 < sp^3 < sp$ in the B complex but $sp^2 \approx sp^3 < sp$ in the Al complex. Obviously, some inconsistencies between the interaction energy and the positive MEP on the π-hole of the triel atom are found for both B and Al complexes. These inconsistencies are partly attributed to strong orbital interaction and large polarization energy.

(3) Solvation not only reinforces the triel bond but affects its nature as well. The interaction strength of both B and Al complexes follows the same order: $sp^3 < sp^2 < sp$. The triel bond in the Al complex varies from an electrostatic interaction in the gas phase to a partially covalent interaction in solvent.

(4) The F substitution in the triel donor also strengths the triel bond and its enhancing effect is related to the number, position, and conformation of F substitution. The F substitution causes a prominent change in the configuration of the complex.

References

1. Schneider HJ (2009) Angew Chem Int Ed 48:3924–3977
2. Scheiner S (1997) Hydrogen bonding: a theoretical perspecitive. Oxford University Press, New York
3. Politzer P, Murray JS, Clark T (2010) Phys Chem Chem Phys 12: 7748–7757
4. Politzer P, Murray JS, Clark T (2013) Phys Chem Chem Phys 15: 11178–11189
5. Politzer P, Murray JS (2013) Chem Phys Chem 14:278–294
6. Guo X, Liu YW, Li QZ, Li WZ, Cheng JB (2015) Chem Phys Let 620:7–12
7. Wei YX, Li QZ, Scheiner S (2018) Chem Phys Chem 19:736–743
8. Grabowski SJ (2014) Chem Phys Chem 15:2985–2993
9. Xu HL, Cheng JB, Yang X, Liu ZB, Li WZ, Li QZ (2017) Chem Phys Chem 18:2442–2450
10. Dong WB, Yang X, Cheng JB, Li WZ, Li QZ (2018) J Fluorine Chem 207:38–44
11. Zierkiewicz W, Michalczyk M, Scheiner S (2018) Molecules 23: 1416
12. Nziko PV, Scheiner S (2016) Phys Chem Chem Phys 18:3581–3590
13. Esrafili MD, Mohammadian-Sabet F (2016) Struct Chem 27:1157–1164
14. Bauzá A, Frontera A (2016) Chem Phys Chem 17:3181–3186
15. Egli M, Gessner RV (1995) Proc Natl Acad Sci USA 92:180–184
16. Hof F, Scofield DM, Schweizer WB, Diederich F (2004) Angew Chem Int Ed 43:5056–5059
17. Zhou P, Zou JW, Tian FF, Shang ZC (2009) J Chem Inf Model 49: 2344–2355
18. Fischer FR, Wood PA, Allen FH, Diederich F (2008) Proc Natl Acad Sci USA 105:17290–17294
19. Kamer KJ, Choudhary A, Raines RT (2013) J Org Chem 78:2099–2103
20. Cormanich RA, Rittner R, O'Hagan D, Bühl M (2016) J Comput Chem 37:25–33
21. Grabowski SJ (2015) Chem Phys Chem 16:1470–1479
22. Leopold KR, Canagaratna M (1997) Acc Chem Res 30:57–64
23. Gao L, Zeng YL, Zhang XY, Meng LP (2016) J Comput Chem 37: 1321–1327
24. Phillips JA, Giesen DJ, Wells NP, Halfen JA, Knutson CC, Wrass JP (2005) J Phys Chem A 36:8199–8208
25. Hase Y (2007) Spectrochim Acta A 68:734–738
26. Müller J, Ruschewitz U, Indris O, Hartwig H, Stahl W (1999) J Am Chem Soc 121:4647–4652
27. Phillips JA, Halfen JA, Wrass JP, Knutson CC, Cramer CJ (2006) Inorg Chem 45:722–731
28. Liu MX, Zhuo HY, Li QZ, Li WZ, Cheng JB (2016) J Mol Model 22:10
29. Esrafili MD, Mohammadian-Sabet F (2016) Mol Phys 114:1528–1538
30. Zhang JR, Wei YX, Li WZ, Cheng JB, Li QZ (2018) Appl Organometal Chem 32:e4367
31. Dong WB, Wang YQ, Yang X, Cheng JB, Li QZ (2018) J Mol Graphics Model 84:118–124
32. Zhang JR, Li WZ, Cheng JB, Liu ZB, Li QZ (2018) RSC Adv 8: 26580–26588
33. Yourdkhani S, Korona T, Hadipour NL (2015) J Comput Chem 36: 2412–2428
34. Grabowski SJ (2018) J Comput Chem 39:472–480
35. Bhunya S, Malakar T, Ganguly G, Paul A (2016) ACS Catal 6: 7907–7934
36. Hamilton CW, Baker RT, Staubitz A, Manners I (2009) Chem Soc Rev 38:279–293
37. Grabowski SJ (2015) Molecules 20:11297–11316
38. Grabowski SJ (2017) Struct Chem 28:1163–1171
39. Jabłoński M (2018) J Comput Chem 39:1177–1191
40. Fiacco DL, Leopold KR (2003) J Phys Chem A 107:2808–2814
41. Bauzá A, Frontera A (2017) Theor Chem Acc 136:37
42. An XL, Liu HP, Li QZ, Gong BA, Cheng JB (2008) J Phys Chem A 112:5258–5263
43. Scheiner S, Grabowski SJ, Kar T (2001) J Phys Chem A 105: 10607–10612
44. Alkorta I, Rozas I, Elguero J (2000) J Fluorine Chem 101:233–238
45. Zou JW, Jiang YJ, Guo M, Hu GX, Zhang B, Liu HC, Yu QC (2005) Chem Eur J 11:740–751
46. Li QZ, Jing B, Li R, Liu ZB, Li WZ, Luan F, Cheng JB, Gong BA, Sun JZ (2011) Phys Chem Chem Phys 13:2266–2271
47. Robertson CC, Wright JS, Carrington EJ, Perutz RN, Hunter CA, Brammer L (2017) Chem Sci 8:5392–5398
48. Shen D, Su PF, Wu W (2018) Phys Chem Chem Phys 20:26126–26139
49. Hansen AS, Du L, Kjaergaard HG (2014) Phys Chem Chem Phys 16:22882–22891
50. Riley KE, Murray JS, Fanfrlík J, Řezáč J, Solá RJ, Concha MC, Ramos FM, Politzer P (2011) J Mol Model 17:3309–3318
51. Boys SF, Bernardi FD (1970) Mol Phys 19:553–556
52. Frisch MJ, Trucks GW, Schlegel HB, Scuseria GE, Robb MA, Cheeseman JR, Montgomery JA Jr, Vreven T, Kudin KN, Burant JC, Millam JM, Iyengar SS, Tomasi J, Barone V, Mennucci B, Scalmani G, Cossi M, Rega N, Petersson GA, Nakatsuji H, Hada M, Ehara M, Toyota K, Fukuda R, Hasegawa J, Ishida M, Nakajima T, Honda Y, Kitao O, Nakai H, Klene MLX, Knox JE, Hratchian HP, Cross JB, Adamo C, Jaramillo J, Gomperts R, Stratmann RE, Yazyev O, Austin AJ, Cammi R, Pomelli C, Ochterski JW, Ayala PY, Morokuma K, Voth GA, Salvador P, Dannenberg JJ, Zakrzewski VGDS, Daniels AD, Strain MC, Farkas O, Malick DK, Rabuck AD, Raghavachari K, Foresman JB, Ortiz JV, Cui Q, Baboul AG, Clifford S, Cioslowski J, Stefanov BB, Liu G, Liashenko A, Piskorz P, Komaromi I, Martin RL, Fox DJ, Keith T, Al-Laham MA, Peng CY, Nanayakkara A, Challacombe M, Gill PMW, Johnson B, Chen W, Gonzalez C, Wong MW, Ittsburgh PA, Pople JA (2009) Gaussian 09, revision A02. Gaussian Inc, Wallingford.
53. Bader RFW (2000) AIM Program, v. 2.0, McMaster University, Hamilton, Canada
54. Bulat FA, Toro-Labbe A, Brinck T, Murray JS, Politzer P (2010) J Mol Model 16:1679–1691
55. Reed AE, Curtiss LA, Weinhold F (1988) Chem Rev 88:899–926
56. Su PF, Li H (2009) J Chem Phys 131:014102
57. Schmidt MW, Baldridge KK, Boalz JA, Elbert ST, Gorden MS, Jensen JH, Koseki S, Matsunaga N, Nguyen KA, Su SJ, Windus TL, Dupuis M, Montgomery JA (1993) J Comput Chem 14:1347–1363
58. SCM, ADF, Release 2008.01; Theoretical Chemistry, Vrije Universiteit, Amsterdam, The Netherlands, Available at: http://www.scm.com
59. Politzer P, Murray JS, Clark T, Resnati G (2017) Phys Chem Chem Phys 19:32166–32178
60. Batsanov SS (2001) Inorg Mater 37:871–885
61. Koch U, Popelier P (1995) J Phys Chem 99:9747–9754
62. Politzer P, Murray JS, Clark T (2015) J Mol Model 21:52
63. Politzer P, Murray JS (2017) Crystals 7:212